Study on polyamide thin film nano-composite membranes using different types of multi-walled carbon nanotubes at different pH feed solutions

Abdel-Hameed Mostafa El-Aassar

Egyptian Desalination Research Center of Excellence (EDRC), Desert Research Center (DRC), Cairo, Egypt.
Tel.:+202-01002501524;+202-26389069, amelaassar@edrc.gov.eg, hameed_m50@yahoo.com.

Abstract: To enhance the performance of polyamide thin film composite (PA-TFC) membranes, non-functionalized, NH2 and COOH functionalized multi-walled carbon nanotubes (MW-CNTs) were used as additives. The PA active layer was prepared via interfacial polymerization between m-Phenylene diamine (MPD) in aqueous phase and trimesoyl chloride (TMC) in dodecane as organic phase. The obtained results indicated a general improvement in the RO performance, the values of permeate flux increased from 33.61 for non-modified PA-TFC membrane to 37.78, 36.15, 38.12 L/m2.h for non-functionalized, NH2, COOH functionalized MW-CNTs, respectively. The obtained TFNC membranes possess high values of salt rejection (%) that is not lower 99.63. The surface hydrophilicity of PA-TFNC membranes improved as compared with the neat PA-TFC membrane. Also, the rejection (R) of both Na+ and Cl-ions showed that at pH< 6.5, at acidic media; the R (Na+) > R (Cl-). On the other hand, at pH > 6.5, at alkaline media the R (Na+) < R (Cl-). While, at pH=6.5, at slightly neutral media; the R (Na+) = R (Cl-).

[Abdel-Hameed Mostafa El-Aassar. **Study on polyamide thin film nano-composite membranes using different types of multi-walled carbon nanotubes at different pH feed solutions.** *J Am Sci* 2016;12(11):52-63]. ISSN 1545-1003 (print); ISSN 2375-7264 (online). http://www.jofamericanscience.org. 5. doi:10.7537/marsjas121116.05.

Key words: Thin film nano-composite membranes; carbon nanotubes; water desalination; reverse osmosis; pH feed solution.

1. Introduction

Desalination is considered as one of the most promising approaches to supply fresh water in the context of a rapidly growing global water gap. Although oceans and seas contain about 97% of the world's water, desalination today only accounts for a fraction of a percent of the world's potable water supply due to large energy footprints and high capital costs [1]. In general, water desalination technologies can be categorized into two basic mechanism separations: thermal and membrane-based water desalination. The thermal processes include multi-stage flash (MSF), multiple effect distillation (MED)and vapor compression distillation (VCD), whereas membrane-based processes include reverse osmosis (RO), nanofiltration (NF), and electrodialysis (ED). Among the water desalination technologies, reverse osmosis (RO) is the primary choice where it dominates up to 44% of the total world desalination capacity [2]. It is the most energy-efficient desalination technique to date with a record of 1.8 kWh/m^3 recently achieved in a commercial plant as compared with an average of 5 kWh/m^3during the 1990 [3]. The evolution of reverse osmosis membranes can be traced to 1959, when Reid and Breton first reported the utility of dense cellulose acetate membranes for desalination [4]. A few years later, Loeb and Sourirajan described the use of asymmetric cellulose acetate membranes, consisting of a thick porous sublayer with only a thin dense skin layer [5]. Francis hypothesized that forming the two layers separately and laminating the dense barrier layer to the porous support would give better performance (i.e. higher permeate flux membranes) and produced the first thin-film composite reverse osmosis membrane in 1964. Problems with the compaction of the microporous cellulose acetate support layer fueled the research to create alternative support layer materials. In 1966; Cadotte developed a method of casting microporous, compaction-resistant Polysulfone support membranes [6]. Polysulfone remains the standard support membrane in the reverse osmosis industry today. Cadotte was also responsible for significant advances in membrane separation layer performance. In 1970, he developed a completely non-cellulosic thin-film composite membrane, containing an aryl-alkyl polyuria barrier layer formed in situ on a microporous Polysulfone support layer [6]. Properties of this membrane, including high permeate flux, high salt rejection, and resistance to biodegradation and compaction, were superior to those of cellulosic membranes, and from that point forward, most improvements in barrier layer materials have centered on the synthetic membranes. Additionally, it opened the door for a wide variety of materials to be considered for the barrier layer [7]. Cadotte and his colleagues prepared polyamide thin film composite (PA-TFC) membranes by interfacial polymerization of trimesoyl chloride and metaphenylene diamine [8]. Many current TFC-RO membranes are based largely

on chemistry similar to that developed by Cadotte [9]. Membrane technology is rapidly growing, improved permeability, selectivity, and antifouling efficiency offer cost and energy effective options for treating water for reuse or safe disposal.

Due to the development of nanotechnology, the researchers have focused on the addition of inorganic nano-materials into the polymeric materials [10, 11] to increase membrane chemical reactivity and reduce fouling [12]. There are two types of nanotechnology enhanced the membrane materials: the mixed matrix membrane (MMM), a mixture of nano-materials (i.e. Filler) in a polymer matrix [13] and a thin film nano-composite (TFNC), the formation of a thin-film layer with fillers on a porous matrix [14]. Both types (MMM and TFNC) enhanced mechanical, physic-chemical stability and reactivity compared with that of common membranes [15]. Among the various nano-materials studied carbon nanotube (CNTs). CNTs have excellent mechanical, electrical, and thermal properties [11] and partial antibacterial properties [16]. CNTs can also alter the physic-chemical properties of a membrane [17]. The inner pores of CNTs act as selective nano-pores, as CNTs composite membranes showed an improved permeability without a decrease in selectivity compared to other types of membrane [18]. Generally, the membrane performance depends on the membrane characteristics and feed water characteristics as well as operating conditions. These variables include applied pressure, temperature and feed water pH [19]. Although most commercial TFC membranes are suitable for treating aqueous streams at a wide pH ranged from 2-10, little is known about the effect of pH on membrane performances and the behavior of both sodium and chloride ions at different pH values [20-22].

The aim of this work is carried out to shed light the effect of different CNTs types doping into the PA barrier layer of TFNC membranes on their performance. The PA barrier layer was prepared via interfacial polymerization technique using the optimum conditions of the previous works [23-25]. The effect of CNTs type and its concentration on the membrane performance and characterization of the obtained TFNC membranes were studied. Also, the second aim of the work included both evaluations of the performance of these prepared TFNC membranes and studying the behavior of Na^+ and Cl^-ions during the desalination processes using different pH feed water solutions.

2. Experimental

2.1. Materials and reagents.

Flat sheet rolls of asymmetric Polysulfone (PSf) support membrane on non-woven polyester fabric were supplied by Dow Water & Process Solutions (Edina, MN). The two monomers included both m-Phenylenediamine (MPD, ≥ 99%) and Trimesoyl chloride (TMC, 98%) were from Sigma-Aldrich (St. Louis, MO). The solvents such as n-dodecane (anhydrous, ≥ 99%) and n-hexane (mixture of isomers, anhydrous ≥ 99%) were used as received from Sigma-Aldrich (St. Louis, MO). The used deionized (DI) water was produced by a Milli-Q Advantage A10 vacuum purification system (Millipore, Billerica, MA). The different types of Multi-wall Carbone nanotubes (MW-CNTs); non-functionalized, COOH rich, NH_2 rich CNTs were supplied from cheap tubes for nano-materials company, USA. These types of MW-CNTs possess an outer diameter ranged from 13-18 nm and length ranged from 3-30 μm, with purity > 99 wt. %. The functional content for the functionalized CNTs types' 7wt. % ±1.5%.

2.2. Preparation of neat and modified polyamide thinfilm nano-composite membranes.

The process of thin film composite membrane preparation was similar to that reported by [23-25]. In brief, the interfacial polymerization process was used to prepare the barrier PA thin layer. The immersing time of PS flat sheet membrane in the MPD aqueous solution was 10 min., while the reaction time between the two monomers; MPD and TMC was 1 min. In case of CNTs incorporation, the CNTs were added in either distilled water or dodecane with sonication for at least 60 min until obtaining homogeneous solutions before the addition of MPD and TMC, respectively. It is very important to mention that, to avoid any defect in the prepared PA-TFC membrane, the residual droplets of MPD aqueous solution on the top surface of the PS membrane were removed before immersing in TMC-dodecane solution by rolling a rubber roller across the membrane surface in one direction. The obtained PA-TFC membrane surface was washed with hexane and left to dry in air at ambient temperature. Finally the prepared membrane was rinsed and immersed in DI water until characterized or used in the water desalination cross-flow experiments.

2.3. Characterization of the obtained polyamide thin-film (PA-TFC) membranes.

The membrane hydrophilicity was studied and evaluated through contact angle measurement. The Oil-in-water contact angle analysis was performed using a Ramé-Hart Model 200-F1 Standard Goniometer with DROP image Standard Edition 2.4 software (Ramé-Hart Instrument Co., Netcong, NJ). Three Strips of each membrane were measured through mounting the strips in sample holder with active side facing down and placed in the DI water bath. N-decane oil droplet was dispensed onto the bottom side of the membrane strip from a Gilmont Instruments 0.2 ml micrometer syringe (Cole-Parmer Instrument Co., Vernon Hills, IL) with a hooked

Hamilton N732 needle (OD: 0.009 in, Hamilton Co., Reno, NV). The contact angle was measured through the water phase, and the reported contact angle is the average value of the left and right side contact angles, at least three oil droplets were placed at different spots in each sample. The smaller angle indicates a more hydrophilic surface.

The chemical structure of the obtained PA-TFC flat sheet membrane was characterized using Attenuated Total Reflectance Fourier Transform Infrared Spectroscopy (ATR-FTIR). The used instrument was Thermo Nicolet Nexus 470 FTIR with an Avatar Smart Miracle ATR accessory and a ZnSe crystal (Thermo Fisher Scientific Inc., Waltham, MA). Spectra were collected in the air, in the mid-infrared region (600-4000 cm^{-1}), using 128 scans at resolution 4. Before and after each measurement, PSf membrane sample was used to make a background spectrum to neglect any atmospheric absorbance peaks.

Also, the membrane top surface and cross-section morphology was characterized by scanning electron microscopyof model of SEM, Zeiss Supra 40 VP, Carl Zeiss NTS, Peabody, MA. High voltage ETH mode was used with voltage of 5 kv. An In Lens detector was selected, and the working distance was between 5 and 7 mm. The tested samples were prepared by peeling away the non-woven polyester backing fabric and fracturing the remaining Polysulfone and polyamide layers after immersion in liquid nitrogen. A Cressington 208 Bench-top Sputter Coater (Cressington Scientific Instruments LTD., Watford, England) having a Pt/Pd metal target was used to coat the samples with coating thickness of 10 nm to ensure adequate sample surface conductivity.

2.4. Reverse Osmosis performance of polyamide thin-film (PA-TFC) membranes.

The performance of the neat prepared PA-TFC and PA-TFNC membranesincorporated with different types of CNTS for water desalination processes was evaluated through measuring both reverse osmosis parameters including; the permeate flux ($L/m^2.h$) and salt rejection (%). Permeate flux and salt rejection were measured using cross-flow filtration unit, as shown in Figure (1).

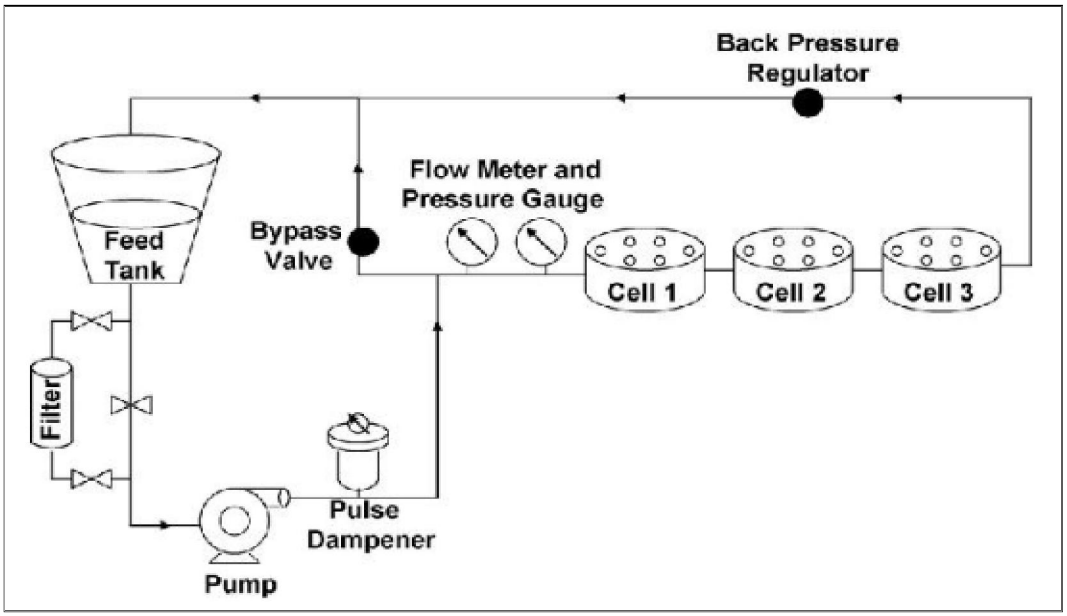

Figure (1) sketch of the used cross-flow filtration unit

The synthesized feed aqueous solutions containing 2000 ppm NaCl were used with different pH range at ambient temperature (25°C). The flow rate was 1G/min and the applied pressure was 225 psi (15.5 bar). All flux and rejection measurements were evaluated after 30 min from the start of the cross-flow experiments to ensure that the filtration process had reached a steady state. The permeate flux (J_W) through a membrane area (A) was calculated as the volume (ΔV) collected during a time period Δt: $J_W = \Delta V / A. \Delta t$

Also, the salt rejection (R_s %) was calculated by measuring the electric conductivity ofboth feed and permeate solutions using an Oakton CON 11 conductivity meter (cole-Parmer Instrument Co., Vernon Hills, IL) and calculated as follows: $R_s\% = (C_f - C_p/C_f) \times 100$.

Where C_f and C_p are the concentrations of the feed and permeate water (product), respectively.

The measuring of both chloride and sodium ions concentrationin the feed or permeate was carried out

using ion chromatography (ICS-2100, Dionex Corp, Sunnyvale, CA).

3. Results and Discussion

3.1. Preparation and characterization of PA-TFNC using different types of CNTs.

In this section, different types of MW-CNTs included non-functionalized and NH_2 as well as COOH-CNTs were doped with the same concentration of (0.01gm) into the PA barrier layer of TFC membranes. The doping was achieved in the two phases; the organic phase (TMC in dodecane solution) or aqueous phase (MPD in distilled water) to shed light on the effect of CNTs doping on the performance of the prepared TFNC membranes and investigate the best phase that the doping will be carried out. The comparison of the different CNTs types based on the reverse osmosis performance; salt rejection (R_S %) and permeate flux (J_{H2O} L/m^2.hr) of the obtained TFNC membranes.

The results of both salt rejection and water flux for the neat and the modified TFNC membrane performance that prepared by CNTs in both organic and aqueous phase are recorded in Tables(1, 2), respectively.

From tables (1,2), It can be seen that, all synthesized included neat PA-TFC and PA-TFNC membranes possess good R_s % indicating that all synthesized membranes have not any defects in the PA-barrier layer. Also, it is obvious that, the doping of MW-CNTs in the organic phase (TMC dodecane solution) improved the R_s % that increased to 99.86 % for both NH_2 and COOH functionalized CNTs with a slight increase in permeate flux. On the other hand, the using of non-functionalized CNTs increased the permeate flux from 33.61 to 38.4 L/m^2.hr with a slight increase in R_s %.

While, the doping in the aqueous phase (MPD aqueous solution) improved the permeate flux that increase from 33.61 for neat PA-TFC membrane to 36.15, 36.75 and 37.78 for PA-TFNC membranes using NH_2-CNTs, COOH-CNTs and NF-CNTs, respectively.

The contact angle of the prepared membranes was measured, as shown in figure (2). It ranged from 33±2 for the neat PA-TFC membrane to 26±1 for COOH-CNTs in aqueous phase doping. In general, the doping with the different types of CNTs in both phases; organic and aqueous phase increased the hydrophilicity, i.e. decreasing the contact angle value by range from 9 up to 21 % of the contact angle value for the neat TFC membrane. The increase in hydrophilicity, i.e. decreasing the contact angle values can be explained due to the tunnel structure of the nanotubes and the functional groups of CNTs such as NH_2 and COOH [26, 27].

Also, the ATR-TIR spectra of PS support layer and the different types of synthesized PA-TFNC membrane surface was shown in figure (3).

The doping of the different types of CNTs was carried out using the same concentration of 0.01 gm in the aqueous phase. It is important to mention that, due to the depth of ATR-RTIR penetration was about 0.4-0.5 µm in the wavelength region of interest [30] and the spectra that reflect from the PA-TFC membrane surface is a combination of polyamide barrier layer (0.1-0.15 µm) and the rest of PS substrate. So, the background baseline was carried out with Polysulfone membrane.

The spectrum of the PS membrane (Fig. 3A), shows peaks at 1587- 1487, 1324, 1294, 1235, 1150-1106cm^{-1} assigned to C-C, C-H, O=S=O (symmetric), C-O-C and O=S=O (asymmetric), respectively.

The spectra of PA-TFC membrane (fig. 3B) shows the absence of the acid chloride band at 1770 cm^{-1}, indicating that successful polymerization has occurred. The bands at 1661 and 1549 cm^{-1} were present, that is characteristic of (amide I) C=O stretching vibrations and amide-II (N–H) band of the amide group (–CONH–). In addition, other bands characteristic of PA occur at 1609.6 and 1488.9cm^{-1} (aromatic ring breathing), and 1250 cm^{-1} (amide III). Also, the stretching peak of OH group was present at 3384 cm^{-1}. This result was in agreement with the previous work of [28]. There is no a reasonable difference between the spectra of both neat PA-TFC (Fig. 3B) and PA-TFNC with NF-CNTs (Fig. 3C). This is due to the low concentration of CNTs and the absence of any function group. On the other hand, there are changes in the spectra of both PA-TFNC membranes using NH_2-CNTs (Fig. 3D) and COOH-CNTs (Fig. 3E). In the spectrum of PA-TFNC membrane using NH_2-CNTs (Fig. 3D), there are slightly shifting in the bands values and an additional band of the amide group band at 1540cm^{-1}. Also, there is a slight decrease in the absorbance of the broad band of the stretching peak of OH group that was present at 3384 cm^{-1}. On the other, the spectrum of PA-TFNC membrane using COOH-CNTs (Fig. 3E), there are increasing in the broadband of the stretching peak of OH group that was present at 3384 cm^{-1}.

Also, both the top membrane surfaces and cross sections for all synthesized membranes were imaged by SEM as shown in Figure (4). From figure (4), it was observed that the PSf porous layer possesses smooth surface (Fig. 4A) as compared with the other synthesized TFC membranes, while the synthesized polyamide TFC surface had a tightly packed globules and scattered ear-shaped polyamide ridges, presumably generated on top of the Polysulfone support layer having surface pores so that MPD could

diffuse into the organic phase to form these micro-protuberances (Fig. 4B).

While in case of doping the different types of CNTs in the PA barrier layer (Figs 4C, 4D, 4E) that corresponding of PA-TFNC membranes using NF-CNTs, NH_2-CNTs and COOH-CNTs, respectively, there is an increase in the surface area and the surface roughness more than that of the neat PA-TFC membrane. This explained why the modified PA-TFNC membranes using CNTs gave higher permeate flux than that of the neat membrane.

In the present work, the improvement of permeate flux was concerned and preferred more than that of R_s % that already possess high values. So, the doping of these different types of CNTs in the aqueous media was concerned in the following experiments. The effect of CNTs concentrations (ranged from 0-0.02 gm) for the three types was studied as shown in the tables (3-5).

In case of using different concentrations from NF-CNTs and NH_2-CNTs, table 3and 4, respectively, there is a deterioration in the membrane performance (R_S and flux) at low concentration of both types of CNTs. By increasing the CNTs concentration, there is an observed improvement in the membrane performance (R_S and flux) until a certain limit. The optimum concentration was 0.01 wt. % for both types of NF-CNTs and NH_2-CNTs. On the other hand, in case of using different concentration of COOH-CNTs, table (5), there is an improvement in the membrane performance (R_S and flux) at very low concentration and the best membrane performance was observed at (0.0025 wt.%). After that, there is a general decrease in the permeate flux with a slight change in the R_s %. So, the best PA-TFNC membrane from each type of MW-CNTs was selected to study the effect of feed water pH on the membrane performance and the behavior of different ions (Na^+ and Cl^-) during the desalination processes. The three selected membranes are;

- M1: using 0.01 NF-CNTs,
- M2: using 0.01 NH_2-CNTs and
- M3: using 0.0025 COOH-CNTs).

3.2 Evaluation of the synthesized PA-TFNC membrane performance at different pH feed water.

In this section, the study was concerned the effect of feed solution pH on the membrane performance and the ions behavior as well as their rejection (%) during the desalination processes at different pH value.

3.2.1 Effect of pH on membrane performance

It is important to mention that, early work on TFC membranes highlighted the effects of operational variables, including feed pressure, temperature, salt concentration, and pH on both water flux and salt rejection [7, 29]. These references stated that; the water flux was independent of feed pH, but salt rejection decreased at extreme pH values (i.e., below pH 5 and above pH 11). Over this pH range, the pH effects were reversible, indicating no permanent change in the membrane structure [30]. In this previous work, the behavior of both water flux and true NaCl rejection as a function of feed pH for three types of commercial PA-TFC membranes; LE, XLE, and AG membranes was studied. The authors stated that; while water flux was independent of feed pH over the pH range considered, rejection increased fairly linearly with increasing feed pH from pH 5-9. The possible explanation for this increasing in rejection seen with increasing pH is the increasingly negative charge on the polyamide membrane surface over this pH range, as indicated by increasingly negative zeta potential values.

On the other hand, another reference [31] showed the effect of pH in the feed water on NaCl solution flux. They found that the flux increases with a decrease in pH value in the feed solution except pH 2. The used type of the membrane is thin film composite for nanofiltration (NF) which prepared by interfacial polymerization between Triethanolamine (TEOA) and trimesoyl chloride (TMC).

From the above mentioned, we can say that there is no a fixed trend or behavior for both flux and salt rejection as a function of pH of the feed solution and the effect of pH on flux and rejection depends mainly on the membrane characteristics. These characteristics include membrane type, membrane iso-electric Point (IEP), the ionizable functional groups, the charge and the pore analysis.

Figures (5, 6) show the effect of pH for the feed water (ranged from 3.5-10.5) on both water flux and salt rejection (%), respectively for the three selected PA-TFNC membranes.

The pH in the solution was adjusted from alkaline to acidic (descending) and from acidic to alkaline (Ascending) to assure the obtained results. This adjustment of pH values was carried out by addition drops from hydrochloric acid (HCl) and sodium hydroxide (NaOH) according to the request pH value. The amount of both HCl and NaOH that was added had a negligible effect on feed concentration, so flux and rejection were calculated without correction for the additional ions. The applied pressure was fixed at 225psi (15.5 bar); the feed TDS was 2000 ppm NaCl solution. From figure (5), interestingly, it was found that the water flux increased with the increase of pH values ranged from 3.5 to 10.5. While, the salt rejection increased with the increase of pH values until a certain limit of pH that equal to 8.5, and then decreased again, as shown in figure (6). The trend of salt rejection increasing as increasing the pH values is the similar trend of the

previous works [7, 29, 30, and 32]. These previous works explained the increasing of salt rejection with pH due to the increasingly negative charge of the polyamide membrane surface over the pH range, as indicated by increasing negative zeta potential values. The only difference between the obtained data with these previous works is that the increasing of salt rejection until pH equal 8.5 after that it decreased again. This may be explained according the effect of pH on the MW-CNTs itself. The effect of pH value on MW-CNTs was studied in the previous work [33], as shown in figure (7). According to this previous work, as the pH values increases, the negative zeta potential of CNTs increase in pH ranged from 4-8.5 after that, the negative zeta potential decreased again.

Table (1): Reverse osmosis performance of the prepared membranes, the doping of CNTs in the organic phase.

Membrane type	CNTs conc. (gm)	Organic phase	
		R_S (%)	J_{H2O} (L/m^2.hr)
Neat PA-TFC	0	99.53	33.61
NF-CNTs	0.01	99.6	38.4
NH_2-CNTs	0.01	99.86	34.49
COOH-CNTs	0.01	99.86	33.6

Table (2): Reverse osmosis performance of the prepared membranes, the doping of CNTs in the aqueous phase.

Membrane type	CNTs conc. (gm)	Aqueous phase	
		R_S (%)	J_{H2O} (L/m^2.hr)
Neat PA-TFC	0	99.53	33.61
NF-CNTs	0.01	99.69	37.78
NH_2-CNTs	0.01	99.58	36.15
COOH-CNTs	0.01	99.58	36.75

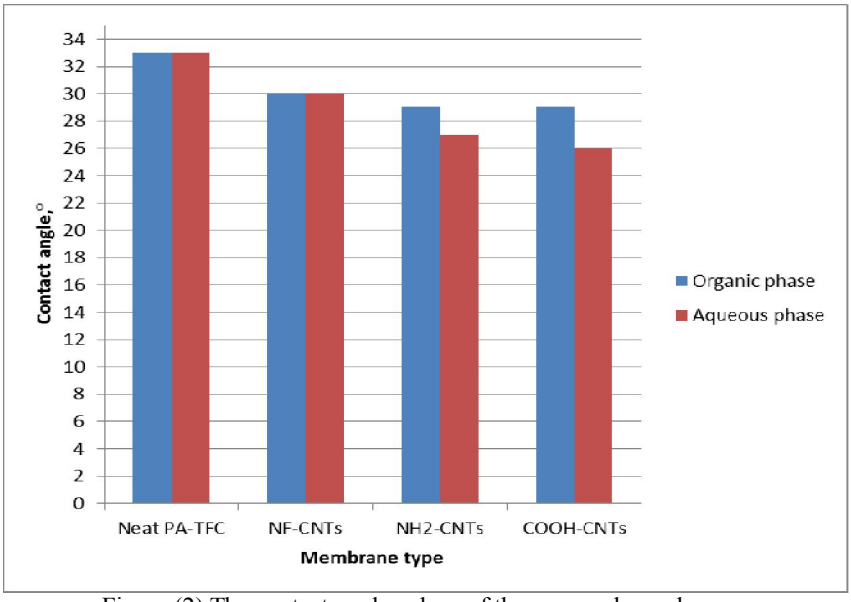

Figure (2) The contact angle values of the prepared membranes

On the other hand, the increase of water flux as a function of pH values can be explained on the base of the effect of pH on CNTs and the nature of liquid transport through CNTs. It was known that, the fluid transport through CNTs is of great interest for research groups since they have been recognized as a promising material for nano-fluidic and membrane technology. The high fluid fluxes reported in the recent publications are contributed by the atomic-scale smoothness of CNTs walls and the molecular ordering phenomena inside the nano-pores [34]. The transport properties of fluid in nano-pores of CNTs depend strongly on the curvature of the surface and shape of the CNTs pores. Solid surfaces have profound influences on the transport properties of as they impart not only normal stresses due to the adsorption potential and the resulting density variation in the direction normal to the interface, but also lateral stresses as demonstrated by Sokhan *et al.* [35] in their simulation studies of fluid flow in nanotubes.

Transport phenomena and density distribution of water molecules under confined and narrow nanotube-channels are important issues since water in various environments demonstrates different properties and the transport mechanism is constrained in many relevant systems. The reduced diameter of CNTs in the order of nanometers has led to differ from those observed in bulk [36]. Additionally, the pore size, molecule-wall interaction and the helicity of CNTs have also made important impacts on the dynamic behaviors and molecular motion of water confined in different nanotubes which in turn determine the transport properties in CNTs [37]. The previous studies [34-38] showed evidence that the absorbed water molecules can exist inside the CNT segments and tend to organize themselves into a highly and long lasting hydrogen-bonded network between adsorbed water molecules. The smooth and frictionless CNT surfaces resulted in weak carbon-water attractive interaction and hence facilitated the extremely high flow velocity. Another important feature revealed by comment consent is the effect of tube diameter, in which the magnitude of the flow rate is reduced by decreasing CNT tube diameter. This characteristic is due to the increase in the average distance between water molecules and carbon atom that resulted in the weakening of water-CNT interaction. The researchers have also conclusively shown that the flow rate could be influenced by some other factors such as the channel structure, water orientation and interatomic distances. A unique combination of the hexagonal structure, water orientations with free OH bonds pointing to the wall and the interatomic distance of 0.142 Å (the C–C bond length of CNTs) has directly affected and rendered great enhancement of flow rate in CNTs. This means that by increasing the alkalinity, i.e, increasing pH values, the most amount of water, orient with the free OH bonds pointing to CNTs wall and increase the water flux.

3.2.2 Effect of pH feed solution on the Na^+ and Cl^- ions behavior

The effect of pH feed solution on the behavior and rejection of Na^+ and Cl^- ions was studied as shown in figure (8). The obtained results with standard deviations ranged from 0-0.0019.

It was obvious that the rejection (%) of ions depends on the pH value of the used feed solution. It was found that; at pH > 6.5, i.e., using neutral to alkaline feed solutions, the R (Na^+) < R (Cl^-). On the other hand, at pH< 6.5, i.e., using the acidic feed solution, the R (Na^+) > R(Cl^-). While at pH=6.5, i.e., using neutral feed solutions, the R (Na^+) = R (Cl^-). Also, the highest R (Na^+, %) which equal to 99.8 % was obtained at feed solution pH =3.5. On the other hand, the highest R (Cl^-, %) which equal to 99.85 % was obtained at feed solution pH =10.5. While at feed solution with pH=8.5, the values of both R (Na^+) and R (Cl^-) were 99.77 and 99.84, respectively. The mechanism of electrostatic repulsion can be employed to explain these obtained results. The surface charge of TFNC membranes possesses more negative as pH increases. This leaded to an increase of electrostatic repulsion that occurred between the Cl^- ions and the negatively charged of the membranes at high pH and vice versa of Na^+ ions at low values of pH.

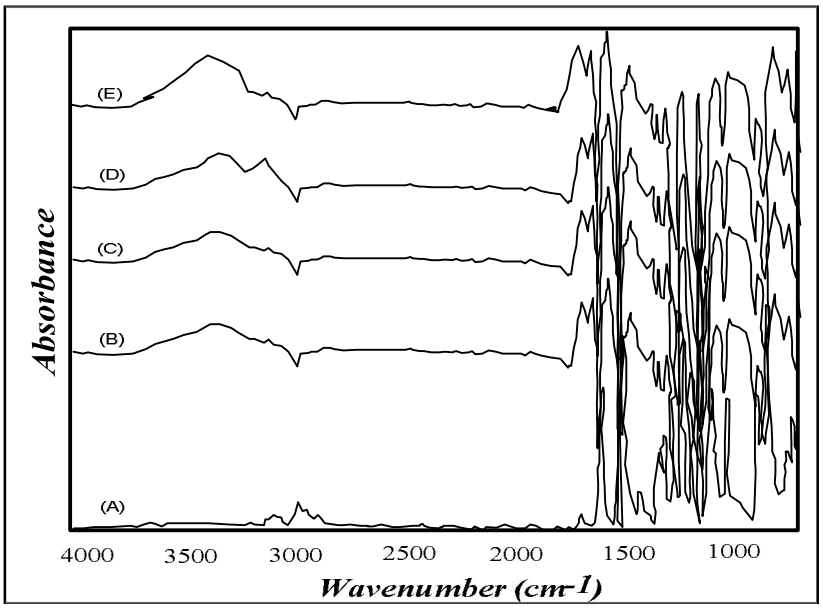

Figure (3) ATR-FTIR of (A) PS, (B) PA-TFC, (C) NF-CNTs PA-TFNC, (D) NH_2-CNTs PA-TFNC and (E) COOH-CNTs PA-TFNC membranes.

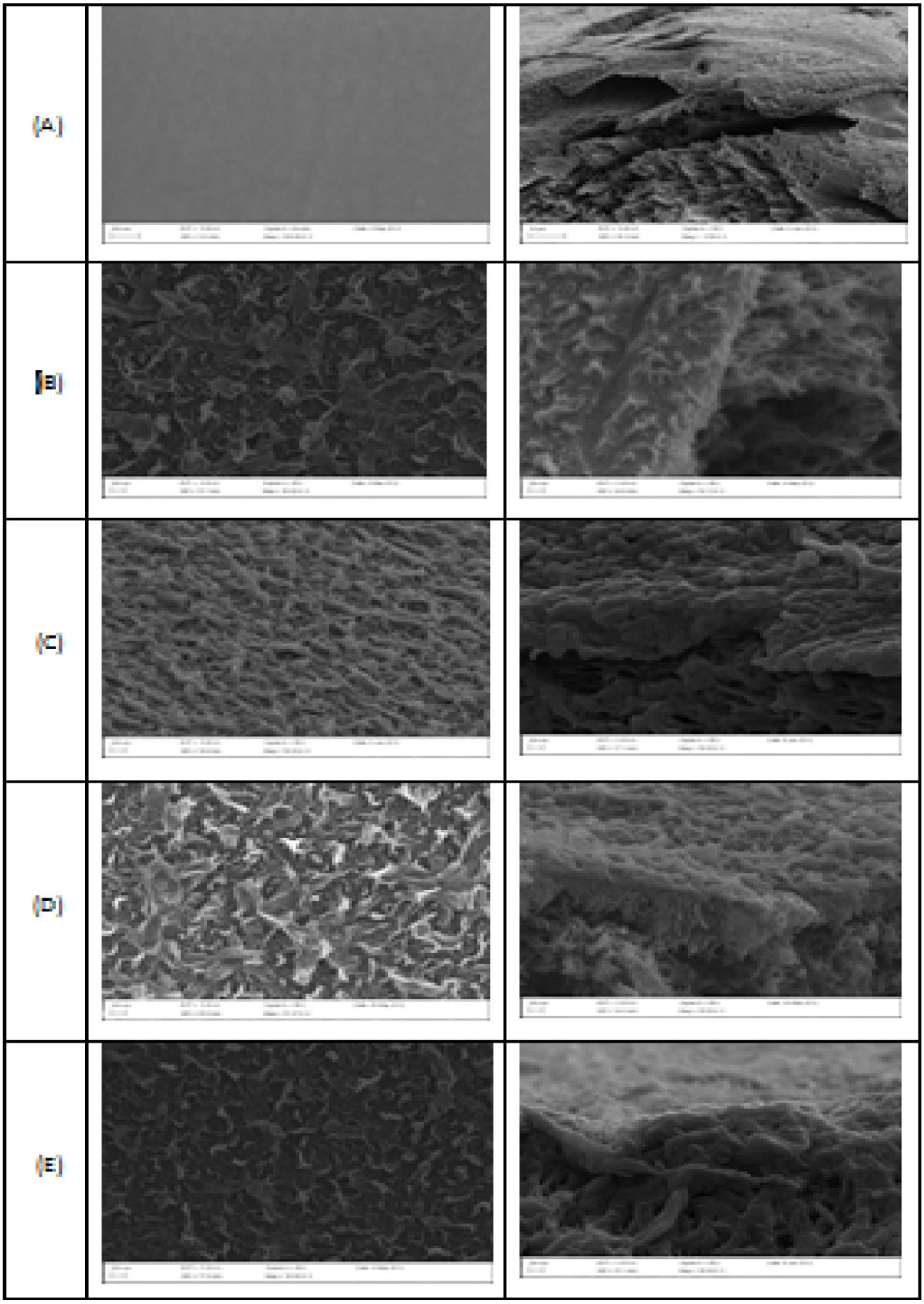

Figure (4) SEM of surface and cross section for TFC and TFNC membranes

Table (3): Effect of non-functionalized CNTs concentration on the reverse osmosis performance of the obtained TFNC membranes.

NF-NTs Conc. (gm)	R_S (%)	J_{H2O} (L/m^2.hr.)
0	99.53	33.61
0.0025	79.54	16.36
0.005	99.42	27.4
0.01	99.69	37.78
0.015	99.32	32.02
0.02	99.6	27.28

Table (4): Effect of NH_2 functionalized CNTs concentration on the reverse osmosis performance of the obtained TFNC membranes.

NH_2-CNTs Conc. (gm)	R_S (%)	J_{H2O} (L/m^2.hr.)
0	99.75	33.61
0.0025	99.26	21.91
0.005	99.67	33.42
0.01	99.68	36.15
0.015	99.79	35.6
0.02	99.79	35.3

Table (5): Effect of COOH-functionalized CNTs concentration on the reverse osmosis performance of the obtained TFNC membranes.

COOH-NTs Conc. (gm)	R_S (%)	J_{H2O} (L/m^2.hr.)
0	99.75	33.61
0.0025	99.63	38.12
0.005	99.69	33.33
0.01	99.58	36.75
0.015	99.68	33.42
0.02	99.75	34.75

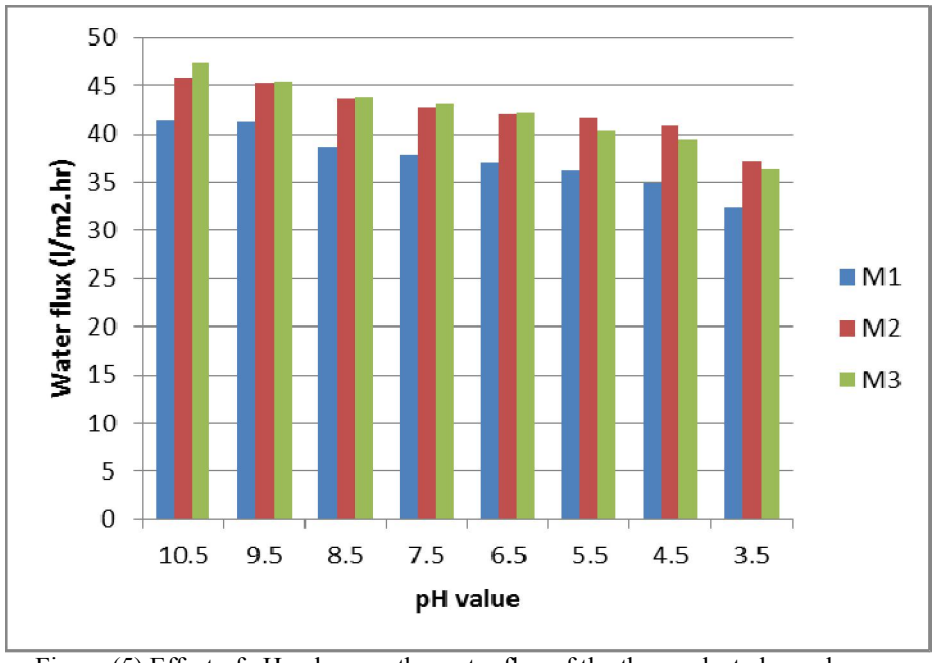

Figure (5) Effect of pH values on the water flux of the three selected membranes

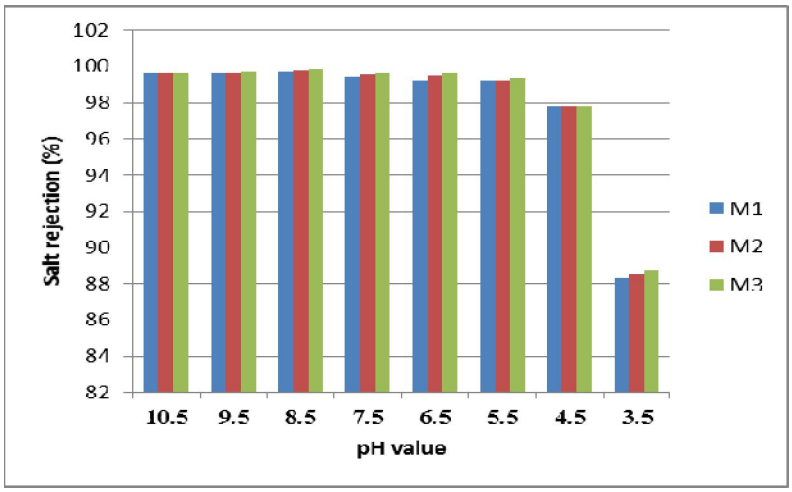

Figure (6) Effect of pH values on the salt rejection (%) of the three selected membranes

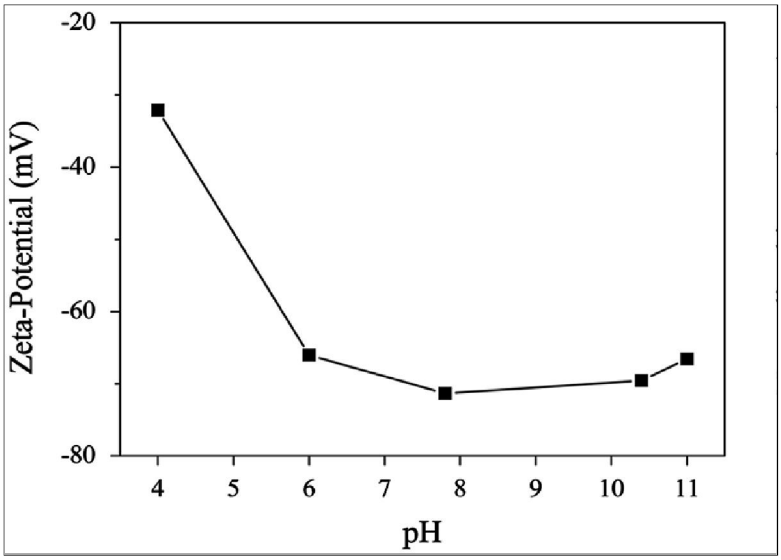

Figure (7): Zeta-potential profile of the MW-CNTs dispersed at different pH values of DI water [33]

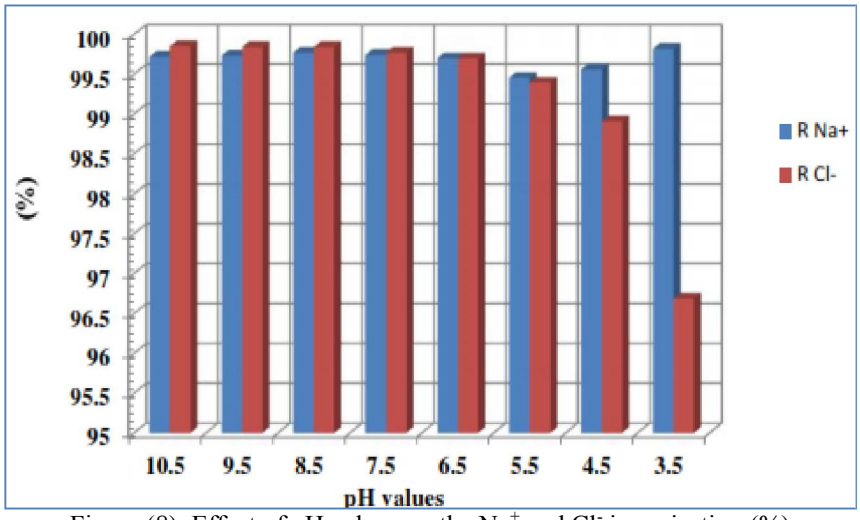

Figure (8): Effect of pH values on the Na^+ and Cl^- ion rejection (%)

4. Conclusions

This study developed new types of TFNC membranes by incorporating different types of CNTs into the PA barrier layer. These types included non-functionalized, NH_2 and COOH Functionalized CNTs. The incorporation was carried out in both organic and aqueous phases. The effect of both CNTs type and its concentration on the membrane performance was studied through the measuring both water flux and salt rejection of the obtained TFNC membranes. Also, their characterization was studied using different instruments such as ATR-FTIR, contact angle measurement and SEM.

By incorporating the different types of CNTs, the obtained membranes become more hydrophilic and possess higher water flux than that of the neat PA-TFC membranewith slightly increasing of salt rejection (%). Also, the effect of pH value on both the RO performance of the three selected membranes and the behavior of ions during the desalination process was studied. Interestingly, it was found that both water flux and salt rejection increased with the increase of pH values. The flux increased as a function of pH ranged from 3.5 to 10.5. While, the salt rejection increased by increasing of pH values until a certain limit that equal to 8.5, and then decreased again. Also, the effect of pH on the ions behavior was studied. The rejection (%) of cation and anion depend on pH values of the feed solution. It was found that at pH > 6.5, the $R(Na^+) < R(Cl^-)$ and at pH=6.5, the $R(Na^+) = R(Cl^-)$, while at pH< 6.5, the $R(Na^+) > R(Cl^-)$.

Acknowledgments

The author thanks Science and Technology Development Fund (STDF, ID 3658) through USA-Egypt Science and Technology collaboration program for supporting his scientific visit in the chemical Engineering Dept., Texas University at Austin, Texas, USA.

Also, the author thanks Prof. Dr. Benny Freeman and all members of his group, especially Joseph Cook.

References

1. Addams L., G. Boccaletti, M. Kerlin, M. Stuchtey Group, 2. W. R., McKinsey and Company Charting Our Water Future: Economic Frameworks to inform Decision-making; 2030 Water resources Group, 2009.
2. Greenlee L.F., D.F. Lawler, B.D. Freeman, B. Marrot, P. Moulin, Reverse osmosis desalination: Water sources, technology, and today's challenges, Water Res. 43 (2009) 2317–2348.
3. Elimelech M., W. A. Phillip, Science (2011), 333, 712-717.
4. Reid C. E., E. J. Breton, Water and ion flow across cellulosic membranes, J. Appl. Polym. Sci., 1(1959) 133-143.
5. Loeb S., S. Sourirajan, Sea water demineralization by means of an osmotic membrane, in: Advances in Chemistry Series, 38 Ed., American Chemical Society, 1963, pp. 117-132.
6. Cadtte J. E., R. J. Petersen, Thin-film composite reverse-osmosis membranes: origin, development, and recent advances, in A. F. Turbak (ed.), Synthetic Membranes: Desalination. ACS Symposium Series, vol. 1, 153 ed., American Chemical Society, 1981, pp. 305-326.
7. Cadotte J. E., R. Paterson, R. E. Larson, E.. Erickson, A new-thin film composite seawater reverse osmosis membrane, Desalination 32 (1980) 25-31.
8. Cadotte J. E., Interfacially synthesized reverse osmosis membranes, U. S. Patent 4, 277, 344, 1981.
9. Van Wagner E. M., A. C. Sagle, M. M. Sharma, B. D. Freeman, Effect of crossflow testing conditions, including feed pH and continuous feed filtration, on commercial reverse osmosis membrane performance, J. of Memb. Sci. 345 (2009),97-109.
10. Yan L., S. Hong, M. L. Li, Y. S. Li, Application of the Al2O3-PVDF nano-composite tubular ultrafiltration (UF) membrane for oily wastewater treatment and its antifouling research, Sep. Purif. Technol. 66 (2009) 347-352.
11. Wu H., B.Tang, P. Wu, MWNTs/polyester thin film nano-composite membrane: an approach to overcome the trade-off effect between permeability and selectivity, J. Phys. Chem. C 114(2010) 16395-16400.
12. Mukhopadhyay S. M., P. Joshi, R. V. Pulikollu, Thin films for coating nanomaterials, Tsinghua Sci. Technol. 10 (2005) 709-717.
13. Kim S., L. Chen, J. K. Johnson, E. Marand, Polysulfone and functionalized carbon nanotube mixed matrix membranes for gas separation: theoryand experiment, J. Membr. Sci. 294 (2007) 147-158.
14. Jeong B. H., E. M. V. Hoek, Y. Yan, A. Subramani, X. Huang, G. Hurwitz, A. K. Ghosh, A. Jawor, Interfacial polymerization of thin film nanocomposite: a new concept for reverse osmosis membranes, J. Membr. Sci. 294 (2007) 1-7.
15. Koros W. J., Evolving beyond the thermal age of separation processes: membranes can lead the way, AIChE. 50 (2004) 2326-2334.
16. Kang S., M. Herzberg, D. F. Rodrigues, M. Elimelech, Antibacterial effects of carbon nanotubes: size does matter, Langmuir 24 (2008) 6409-6413.
17. Brunet L., D. Y. Lyon, K. Zodrow, J. C. Rouch, B. Caussat, P. Serp, J. C. Remigy, M. R. Wiesner, P. J. J. Alvarez, Properties of membranes containing semi-dispersed carbon nanotubes, Environ. Eng. Sci. 25 (2008) 565-576.
18. Kim S., J. R. Jinschek, H. Chen, D. s. Sholl, E. Marand, Scalable fabrication of carbone nanotubes /

polymer nanocomposite membranes for high flux gas transport, Nano Lett. 7 (2007)2806-2811.
19. Van Wagner E. M., A. C. Sagle, M. M. Sharma, B. D. Freeman, Effect of crossflow testing conditions, including feed pH and contious feed filtration, on commercial reverse osmosis membrane performance, J. of Membr sci., 345 (2009) 97-109.
20. Dalwani M., N. E. Benes, G. Bargeman, D. Stamatialis, M. Wessling, Effect of pH on the performance of polyamide /polyacrylonitrile based thin film composite membranes, J. of Membr Sci., 372 (2011) 228-238.
21. Vandezande P., L. E. M.Gevers, L. F. J. Vankelecom, Solvent resistant nano-filtration: separation on a molecular level, Chemical Sociaty Reviews (2008).
22. Schafer A.S. I., A. G. Fane, T. D. Waite, Nanofiltration- principles and applications, Elsevier, 2005.
23. El-Aassar A. M., Improvement of reverse osmosis performance of polyamide thin-film composite membranes using TiO_2 nanoparticles, Desalination and water treatment, (2014), 1-12.
24. Mitchell G.E., B. Mickols, D. Hernandez-Cruz, A. Hitchcock, "Unexpected new phase detected in FT30 type reverse osmosis membranes using scanning transmission X-ray microscopy, Polymer 52 (2011) 3956-3962.
25. Xie W., G. M. Geise, B. D. Freeman, L. Hae-Seung, G. Byun, J. Mcgrath, "Polyamide interfacial composite membranes prepared from m-phenylene diamine, trimesoyl chloride and a new disulfonated diamine", Journal of Membrane Science, Volumes 403–404, 1 (June 2012), Pages 152-161.
26. Saito T., K. Matsushige, K. Tanaka, "Chemical treatment and modification of multi-walled carbon nanotubes", Physica B 323 (2002) 280-283.
27. Kim E., G. Hwang, M. Gamal El-Din, Y. Liu, "Development of nano-silver and multi-walled carbon nanotubes thin-film nano-composite membrane for enhanced water treatment", J. of Membr. Sci. 394-395 2012) 37-48.
28. El-Aassar A. M., "Polyamide Thin Film Composite Membranes Using Interfacial Polymerization: Synthesis, Characterization and Reverse Osmosis Performance for Water Desalination", Australian Journal of Basic and Applied Sciences, 6(6), (2012), 382-391, ISSN 1991-8178.
29. Larson R. E., Cadotte J. E., Peterson R. J., "Development of the FT-30 thin film composite membrane for sea water desalting applications, NWSIA J. 8 (1981) 15-25.
30. Van-Wagner E. M., Sagle A. C., Sharma M. M., Freeman B. D., "Effect of crossflow testing conditions, including feed pH and continuous feed filtration, on commercial reverse osmosis membrane performance", J. of Membr. Sci. 345 (2009) 97-109.
31. Tang B., Z. Huo, P. Wu, "Study on a novel polyester composite nanofiltration membrane by interfacial polymerization of triethanolamine (TEOA) and trimesoyl chloride (TMC): I. reparation, characterization and nano-filtration properties test of membrane, J. of Membra. Sci., 320 (2008) 198-205.
32. Elimelech M., W. H. Chen, J. J. Waypa, "Measuring the zeta (electrokinetic) potential of reverse osmosis membranes by a streaming potential analyzer, Desalination 95 (1994) 269-286.
33. Kunli Goh, Laurentia Setiawan, LiWei, Wenchao Jiang, Rong Wang, Yuan Chen, "Fabrication of novel functionalized multi-walled carbon nanotube immobilized hollow fiber membranes for enhanced performance in forward osmosis process", Journal of Membrane Science 446 (2013) 244–254.
34. Konduri S., H.M. Tong, S. Chempath, S. Nair, J. Phys. Chem. C 112 (2008)15367–15374.
35. Sokhan V.P., D. Nicholson, N. Quirke, J. Chem. Phys. 117 (18) (2002) 8531–8539.
36. Yarin A.L., A.G. Yazicioglu, C.M. Megaridis, M.P. Rossi, Y. Gogotsi, J. Appl. Phys.97 (124309) (2005) 1–13.
37. Liu Y., Q. Wang, L. Zhang, T. Wu, Langmuir 21 (2005) 12025–12030.
38. Ismail A.F., P.S. Goh, S.M. Sanip, M. Aziz, "Transport and separation properties of carbon nanotube-mixed matrix membrane", Separation and Purification Technology 70 (2009) 12–26.

11/6/2016